European Review for Medical and Pharmacological Sciences 2020; 24: 9333-9342

The circular RNA circPTK2 inhibits EMT in hepatocellular carcinoma by acting as a ceRNA and sponging miR-92a to upregulate E-cadherin

T.-T. GONG[1,2], F.-Z. SUN[3], J.-Y CHEN[1], J.-F. LIU[1], Y. YAN[2], D. LI[2], B. ZHOU[1,2], H. SHAN[1,2]

[1]Department of Interventional Medicine, The Fifth Affiliated Hospital of Sun Yat-Sen University, Zhuhai, Guangdong, China
[2]Guangdong Provincial Engineering Research Center of Molecular Imaging, The Fifth Affiliated Hospital of Sun Yat-Sen University, Zhuhai, Guangdong, China
[3]Department of Biotherapy, State Key Laboratory of Oncology in Southern China, Collaborative Innovation Center for Cancer Medicine, Sun Yat-Sen University Cancer Center, Guangzhou, Guangdong, China

Tingting Gong and Fengze Sun have contributed equally to this work

Abstract. – OBJECTIVE: Hepatocellular carcinoma (HCC) is a common malignant tumor. Increasing evidence has demonstrated that microRNAs (miRNAs) play an important role in a wide variety of cellular processes. However, there are few reports about the role and underlying molecular mechanisms of miRNAs in HCC.

PATIENTS AND METHODS: qRT-PCR and Western blots were performed to quantify the expression of miR-92a, E-cadherin, and circPTK2. Proliferation and invasion assays were performed to explore the function of miR-92a and circPTK2. A Luciferase assay was used to test the relationship between miR-92a, E-cadherin, and circPTK2.

RESULTS: In this study, we found that miR-92a was upregulated in HCC tissues and HCC cell lines. Overexpression of miR-92a enhanced cell proliferation and invasion by targeting the E-cadherin 3′UTR in HCC cells. Furthermore, we found that circPTK2 inhibited EMT by inhibiting miR-92a, preventing its ability to downregulate E-cadherin in HCC cells.

CONCLUSIONS: We identified a regulatory axis comprising circPTK2/miR-92a/E-cadherin in HCC cells that may serve as a valuable biomarker and therapeutic target for patients with HCC.

Key Words:
MicroRNA, CircRNA, EMT, Hepatocellular carcinoma, Competing endogenous RNAs.

Introduction

In 2018, liver cancer was the sixth most commonly diagnosed cancer and the fourth leading cause of cancer death worldwide[1]. Hepatocellular carcinoma (HCC) accounts for 80% of liver cancers. Many factors affect the prognosis of patients with hepatocellular carcinoma, but metastasis stands out as the most clinically challenging development[2]. An increasing number of molecular mechanisms of metastasis is currently being investigated, but the role of networks between mRNAs and non-coding RNAs (ncRNAs) remains an area of uncertainty. ncRNAs such as microRNAs (miRNAs) and circular RNAs (circRNAs) are deeply involved in the carcinogenesis, immune escape, metastasis, and drug resistance of tumors[3-5].

MiRNAs are short non-coding RNAs that regulate approximately 60% of the human protein-coding genes and regulate the expression of proteins associated with most biological processes[6]. Intriguingly, circRNAs may compete with endogenous RNAs (ceRNAs) and interact with mRNAs by competitively binding their common miRNAs[7,8]. MiR-92a-3p is a core member of the miR-17-92 cluster, which is especially overexpressed in human cancers and has been suggested to participate in the onset and progression of cancer[9]. E-cadherin is an important cell adhesion molecule in the epithelial-mesenchymal transition (EMT). In this process, E-cadherin expression is decreased, and N-cadherin is increased. Moreover, epithelial cells transform into mesenchymal phenotype cells [10,11]. The cytoskeleton,

Corresponding Authors: Dan Li, email: 479782767@qq.com
Bin Zhou, email: zhoub2@mail.sysu.edu.cn

typically composed of cytokeratin in epithelial cells, transforms to be comprised primarily of vimentin, which is characteristic of mesenchymal cells[12]. Through EMT, epithelial cells lose their polarity and connections with the basement membrane and other epithelial phenotypes and acquire interstitial phenotypes such as higher migration and invasion, extended survival, and the expression of metalloproteinases (MMP) that give them the ability to degrade the extracellular matrix[13,14]. Of interest, MMP-2 and MMP-9 are positively associated with the expression of claudin-4 (CLDN4)[15]. However, the mechanism by which E-cadherin expression is reduced during the progression of HCC remains unclear.

In this study, we identified miR-92a-3p as an oncogene in HCC that targets E-cadherin, reducing its expression. We also found that circPTK2, also named hsa_circ_0008305, inhibited the progression and metastasis of HCC through the circPTK2/miR-92a/E-cadherin axis.

Patients and Methods

Clinical Samples and Cell Lines

Matched HCC tissues and adjacent tissues from 6 HCC patients undergoing hepatectomy were acquired from the Fifth Affiliated Hospital of Sun Yat-sen University (Zhuhai, Guangdong, China). Hep3B, Huh7, and HepG2 HCC cells were purchased from the American Type Culture Collection (ATCC, Manassas, VA, USA). LO2, MHCC-97L, Bel-7402, and SMMC-7721 cells were purchased from the Shanghai Institute of Cell Biology (SICB, China). All cells were cultured in Dulbecco's Modified Eagle Medium (DMEM; Gibco, Grand Island, NY, USA) supplemented with 10% fetal bovine serum (FBS) (Gibco, Grand Island, NY, USA) and 1% penicillin/streptomycin. All cells were cultured in a humidified incubator at 37°C with 5% CO_2. Approval was acquired from the Research Ethics Committee of the Fifth Affiliated Hospital of Sun Yat-sen University.

Transfection

MiR-92a mimic (miR-92a MI), mimic negative control (MI NC), miR-92a inhibitor (miR-92a IN), and inhibitor negative control (IN NC) were purchased from RiboBio (Guangzhou, China). Cells were transfected with Lipofectamine® 2000 (Invitrogen, Carlsbad, CA, USA) following the manufacturer's protocol.

RNA Isolation and Real-Time qRT-PCR

Total RNA containing miRNA and mRNA was extracted from tissue samples and cells using an HP Total RNA Kit (Omega, Norcross, GA, USA). cDNA synthesis was performed using a miRNA First-Strand Synthesis Kit (TaKaRa, Dalian, Liaoning, China) and a PrimeScript™ RT reagent kit (TaKaRa, Dalian, Liaoning, China) according to the manufacturer's instructions. The expression of mRNA was detected by using TB Green™ Premix Ex Taq II (TaKaRa, Dalian, Liaoning, China) according to the manufacturer's instructions with the CFX96 Real-Time PCR Detection System (Bio-Rad, Hercules, CA, USA). The relative expression of mRNAs or miRNAs was normalized to glyceraldehyde 3-phosphate dehydrogenase (GAPDH) or snRNA U6 expression, respectively, and was calculated using the $2^{-\Delta\Delta CT}$ method. The primers used were: E-cadherin, forward: 5′-GAACGCATTGCCACATACAC-3′ and reverse: 5′-GAATTCGGGCTTGTTGTCAT-3′; N-cadherin, forward: 5′-CCTGAGGGATCAAAGCCTGGAAC-3′ and reverse: 5′-TTGGAGCCTGAGACACGATTCTG-3′; Vimentin, forward: 5′-AGTCCGCACATTCGAGCAA-3′ and reverse: 5′-GGGGAAACCGTTAGACCAGAT-3; MMP2, forward: 5′-TACAGGATCATTGGCTACACACC-3′ and reverse: 5′- GGTCACATCGCTCCAGACT-3′; MMP9, forward: 5′-CGAACTTTGACAGCGACAAGA-3′ and reverse: 5′-TCAGGGCGAGGACCATAGAG-3′; CLDN4, forward: 5′- TGCCTGGAGGATGAAAGCG-3′ and reverse: 5′-GAAGTCTTGGATGATGTTGTGGG-3′; GAPDH, forward: 5′-AGAAGGCTGGGGCTCATTTG-3′ and reverse: 5′-AGGGGCCATCCACAGTCTTC-3′; miR-92a, forward: 5′-TGCACTTGTCCCGGCCTGT-3′; and circPTK2, forward: 5′-GCCAAAACACTAAGAAAACTGATCC-3′ and reverse: 5′-ACCAAGAGCACACTTGAAGCAT-3′. All experiments were repeated three times and results were normalized to the control.

Protein Extraction and Western Blotting

Cells were lysed in radioimmunoprecipitation assay (RIPA) Lysis Buffer (Beyotime, Beijing, China) supplemented with phenylmethylsulfonyl fluoride. Protein concentrations were quantified with a bicinchoninic acid (BCA) protein assay kit (Beyotime, Beijing, China). Equal amounts of protein lysates (30 μg per lane) were separated on a 10% sodium dodecyl sulfate-polyacrylamide gel electrophoresis (SDS-PAGE) gel and then transferred to polyvinylidene difluoride

(PVDF) membranes (Millipore, Billerica, MA, USA). The membranes were blocked with 5% nonfat milk in TBST and then incubated with primary antibodies overnight at 4°C. After extensive washing, the membrane was incubated with a secondary antibody conjugated to horseradish peroxidase (Santa Cruz Biotechnology, Santa Cruz, CA, USA) for 1 h at room temperature. The proteins were detected via a chemiluminescent detection system (Thermo Scientific, Waltham, MA, USA) and exposed in a Molecular Imager ChemiDoc XRS (Bio-Rad, Hercules, CA, USA). Protein levels were normalized to GAPDH. GAPDH (2118S), MMP-2 (87809S), and vimentin (5741S) antibodies were purchased from Cell Signaling (Cell Signaling Technology, Danvers, MA, USA). E-cadherin (A11492), N-cadherin (A3045), MMP-9 (A2095), and CLDN4 (A12912) antibodies were obtained from ABclonal (Wuhan, Hubei, China).

Invasion Assays

Cells in serum-free medium (1×10^5 cells/100 μL) were added to the top chamber of a 8-μm-pore Transwell chamber (Corning Star, Chemung, NY, USA) coated with Matrigel® (BD Biosciences, Franklin Lakes, NJ, USA). DMEM containing 10% FBS was added to the lower chamber as the chemoattractant. Cells were allowed to migrate through the porous membrane for 24 h at 37°C in a humidified incubator with 5% CO_2. The cells remaining on the upper membrane were removed by cotton swabs, and those that stuck to the lower surface of the membrane were fixed in 4% paraformaldehyde and stained with 0.1% crystal violet (Beyotime, Beijing, China). The number of invading cells on the lower surface of the membrane was counted at five randomly selected fields in three independent inserts.

Cell Proliferation Assay

A Cell Counting Kit-8 (CCK-8, Dojindo Chemical Laboratory, Kumamoto, Japan) was used to quantify cell proliferation. Approximately 5×10^3 cells in 100 μL medium were seeded into 96-well plates after transfection. After incubation at 37°C for 2 h, the absorbance at 450 nm was measured following the addition of 10 μL of the CCK-8 solution. There were 5 replicates for each group, and 3 independent experiments were performed.

Luciferase Assays

Wild-type or mutant circPTK2 or 3'-UTR of E-cadherin were PCR-amplified and subcloned into the pEZX-MT06 vector to construct the pEZX-MT06-circPTK2 vector or the pEZX-MT06-E-cadherin-3'UTR vector, respectively. 293T cells were seeded in 24-well plates 24 h before transfection. Afterward, 500 ng of pEZX-MT06-circPTK2 vector, pEZX-MT06-E-cadherin-3'UTR vector, or pEZX-MT06 vector, with the addition of 50 nM of miRNA mimic or mimic negative control, were co-transfected into cells using Lipofectamine™ 2000 (Invitrogen, Carlsbad, CA, USA). After 48 h, Luciferase activity was detected with a Dual-Luciferase Assay Kit (Promega, Madison, WI, USA). The relative Luciferase activity was normalized to a standard (Renilla Luciferase activity).

Statistical Analysis

GraphPad Prism 7.0 (GraphPad Software, San Diego, CA, USA) and SPSS software version 20.0 (SPSS Inc., Armonk, NY, USA) were used for data analyses. The experimental results were expressed as means ± SD. Comparisons between groups were conducted using unpaired Student's *t*-tests. The statistical significance was indicated as $*p<0.05$, $**p<0.01$, or $***p<0.001$.

Results

A Screen of MiRNAs Differentially Expressed Between HCC and Adjacent Specimens

To explore the role of miRNAs in HCC, we first analyzed differential miRNA expression form The Cancer Genome Atlas database (TCGA). We found upregulated expression of miR-92a in HCC (n=375) than normal tissues (n=50) (Figure 1A). To validate this result, we detected miR-92a expression in our 6 pairs of HCC and adjacent tissues via qRT-PCR. We found that the expression of miR-92a in HCC tissues was significantly higher than in adjacent healthy tissues (Figure 1B). To verify whether miR-92a is also overexpressed in HCC cell lines, we tested the expression of miR-92a in 6 HCC cell lines, MHCC-97L, Huh7, Bel-7402, Hep3B, HepG2, and SMMC-7721 and in the non-cancerous human liver cell line LO2. We found that miR-92a expression was significantly upregulated in the 6 HCC cell lines compared with LO2 (Figure 1C), in good agreement with our findings from actual HCC tissue. These results suggested that miR-92a may be involved in the development of HCC.

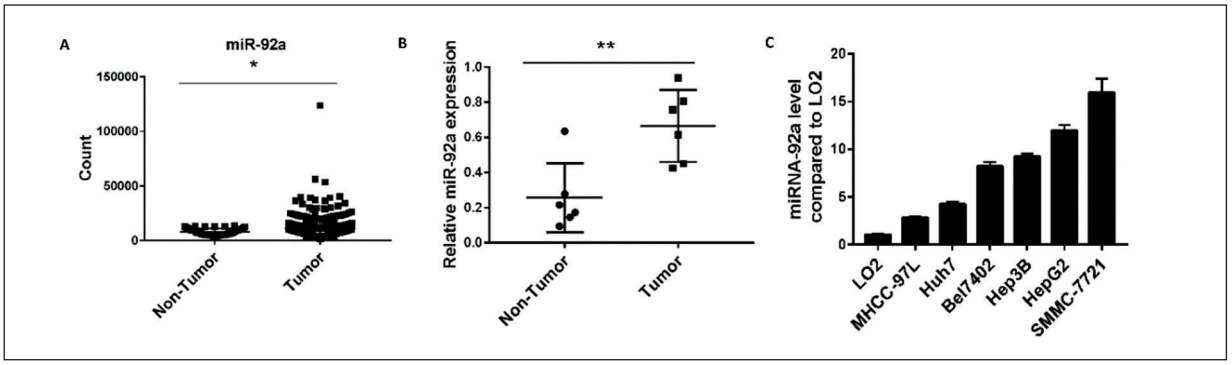

Figure 1. miR-92a is upregulated in HCC tissues and cell lines. **A,** Relative expression levels of miRNA-92a in HCC tissues (n=375) and in adjacent healthy tissues (n=50). **B,** Relative expression of miRNA-92a from 6 paired HCC tissues and adjacent healthy tissues, measured using qRT-PCR; miRNA-92a expression was significantly upregulated in HCC tissues compared to adjacent healthy tissues. **C,** The expression of miRNA-92a was upregulated in HCC cells, including MHCC-97L, Huh7, Bel-7402, Hep3B, HepG2, and SMMC-7721 cells, compared to the nonmalignant LO2 hepatocytes. *p <0.05; **p<0.01.

MiR-92a Promotes Cell Proliferation and EMT of HCC In Vitro

To test the role of miR-92a in HCC proliferation and metastasis, miR-92a MI and miR-92a IN were transfected into Hep3B and MHCC-97L cells. We found that the expression of miR-92a was significantly upregulated or downregulated compared with the MI NC via qRT-PCR (Figure 2A and B). Subsequently, we investigated the role of miR-92 on HCC cell proliferation by using a CCK-8 assay. Intriguingly, increased miR-92a markedly promoted cell proliferation in both Hep3B and MHCC-97L cells, and miR-92a knockdown inhibited cell proliferation (Figure 2C and D). Moreover, cell invasiveness in both HCC cell lines was significantly increased by miR-92a overexpression and suppressed by miR-92a knockdown, as shown in transwell assays (Figure 2E and F).

E-cadherin is a Direct Target of MiR-92a in HCC Cells

To further characterize the molecular mechanisms behind the oncogenic role of miR-92a in HCC cells, a bioinformatics analysis was performed using the starBase v3.0, miRTarBase, and TargetScan databases, which predicted that E-cadherin and CHCHD10 may be biological targets of miR-92a (Figure 3A). E-cadherin was selected for further study because E-cadherin was associated with poor prognosis of HCC and higher propensity for EMT. The predicted binding sites of miR-92a in the E-cadherin sequence are shown in Figure 3B. To determine whether E-cadherin is a direct target of miR-92a in HCC cells, a Luciferase reporter gene assay was performed. The results showed that miR-92a overexpression significantly inhibited the Luciferase activity of the wild-type E-cadherin 3'UTR, while the activity of the mutant E-cadherin 3'UTR remained unchanged (Figure 3C). Next, qRT-PCR and Western blot analyses confirmed that overexpression of miR-92a significantly inhibited the expression of E-cadherin at the protein level in Hep3B cells. In good agreement with this finding, knockdown of miR-92a promoted the expression of MMP2, vimentin, MMP9, N-cadherin, and CLDN4 at the protein level in Hep3B cells (Figure 3D and E).

CircPTK2 Positively Regulates E-cadherin Expression by Sponging MiR-92a in HCC Cells

We next explored the underlying mechanism by which miR-92a regulates HCC progression. Increasing evidence suggests that circRNAs can act as ceRNAs to competitively bind microRNAs. To examine whether miR-92a has a similar mechanism in HCC, we used the starBase online tool to explore the association between miR-92a and circRNAs. To analyze whether circPTK2 acts as a ceRNA to mediate the regulation of miR-92a, we performed a Dual-Luciferase reporter assay in 293T cells. The Luciferase activity of wild-type circPTK2 (circPTK2 wild) was reduced by the miR-92a mimic. However, the Luciferase activity of mutant circPTK2 (circPTK2 mut) was nearly unchanged (Figure 4A and B). Furthermore, the

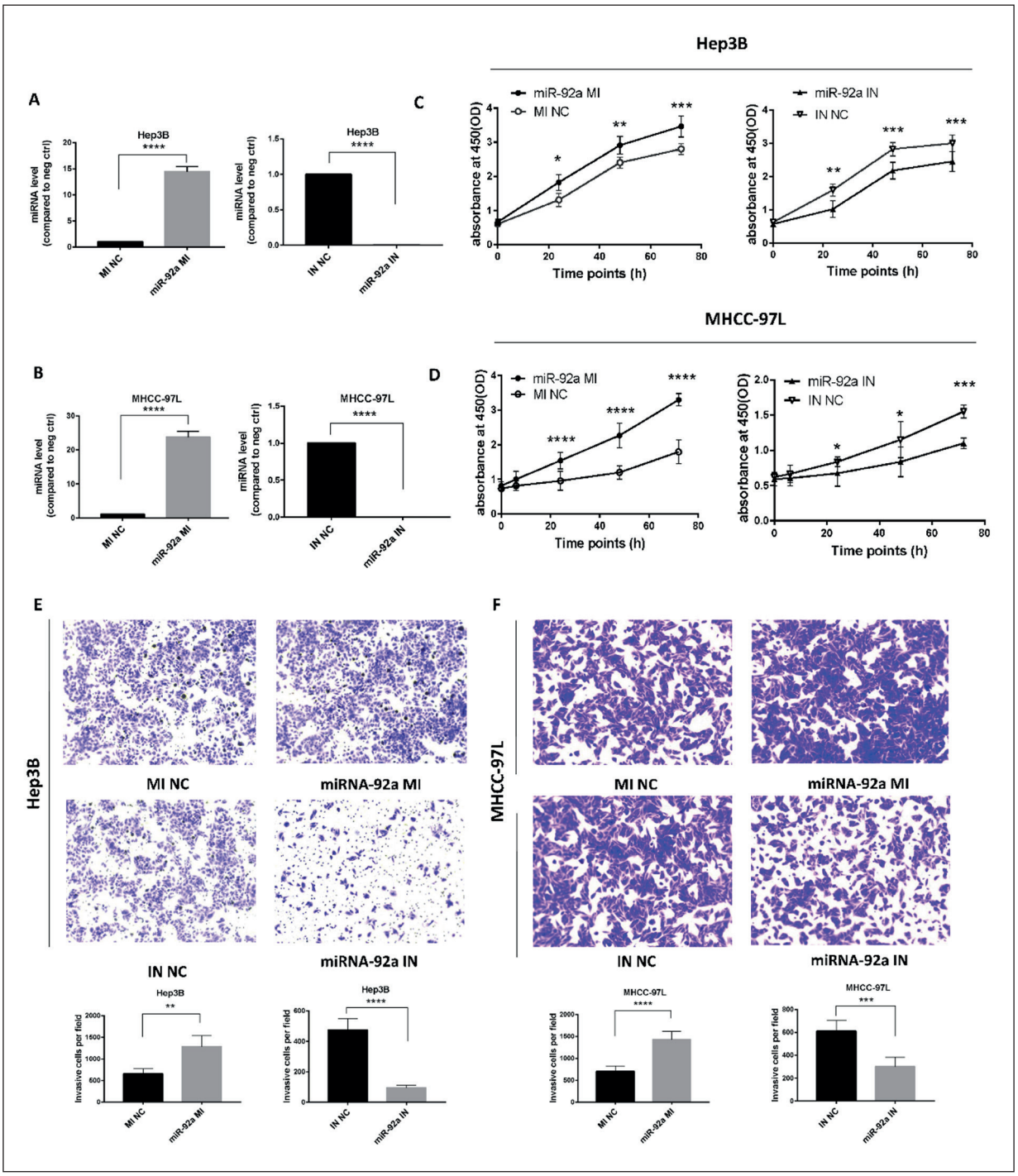

Figure 2. MiRNA-92a affects the proliferative and invasive capacity of HCC cell lines *in vitro*. **A,** and **B,** miR-92a mimic and miR-92a inhibitor were transfected into Hep3B and MHCC-97L cell lines, and the expression of miR-92a was analyzed via qRT-PCR. **C,** and **D,** After transfection with miR-92a mimic or miR-92a inhibitor, the cell viability of Hep3B and MHCC-97L cells was determined using CCK-8 assays. **E,** and **F,** The invasive activity of cells transfected with miR-92a mimic or inhibitor was evaluated by the transwell assay in Hep3B and MHCC-97L cells (200×). *p <0.05; **p < 0.01; ***p< 0.001; ****p< 0.0001.

overexpression of circPTK2 significantly reduced miR-92a expression (Figure 4C) but increased the mRNA expression (Figure 4D) and protein expression (Figure 4E) of E-cadherin in Hep3B cells and MHCC-97L cells. In summary, our results showed that circPTK2 upregulated the

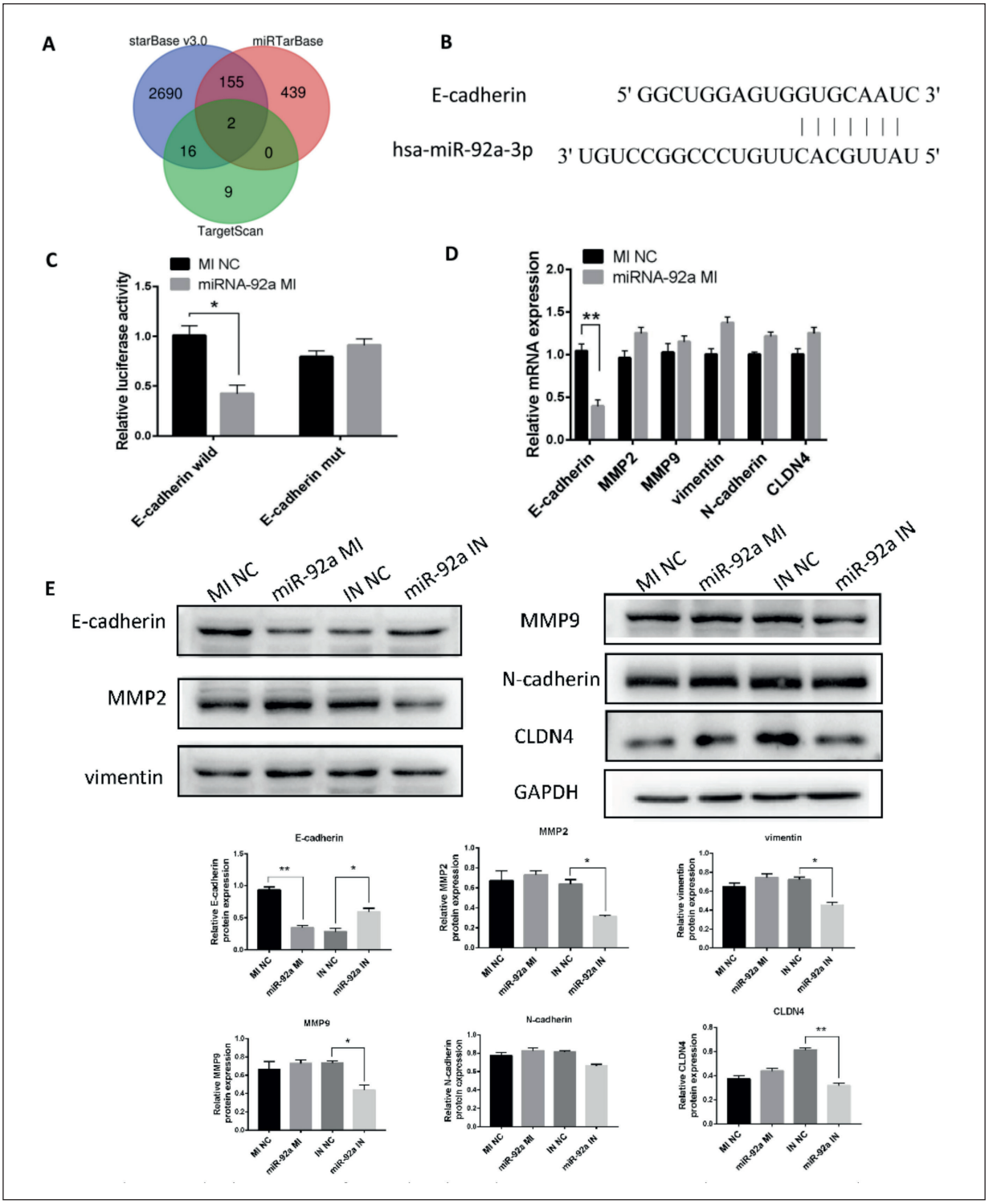

Figure 3. A, *In silico* analysis was performed using the starBase v3.0, miRTarBase, and TargetScan databases, and joint data analysis predicted that two mRNAs (E-cadherin and CHCHD10) may be biological targets of miR-92a. **B,** The putative miR-92a-binding sequence within the 3'UTR of E-cadherin mRNA. **C,** Reporter plasmids containing either the wild-type 3'UTR or a mutated 3'UTR of the E-cadherin gene were co-transfected into 293T cells with an miR-92a-encoding plasmid, and Luciferase activity was measured. WT, wild type; MUT, mutant. **D,** qRT-PCR analysis of relative mRNA levels in Hep3B cells overexpressing miR-92a. **E,** Western blot analysis of relative protein expression in Hep3B cells transfected with miR-92a mimic or inhibitor. Cells transfected with a control mimic (MI NC) or inhibitor (IN NC) plasmids were used as a control. *p <0.05; **p < 0.01; ***p < 0.001.

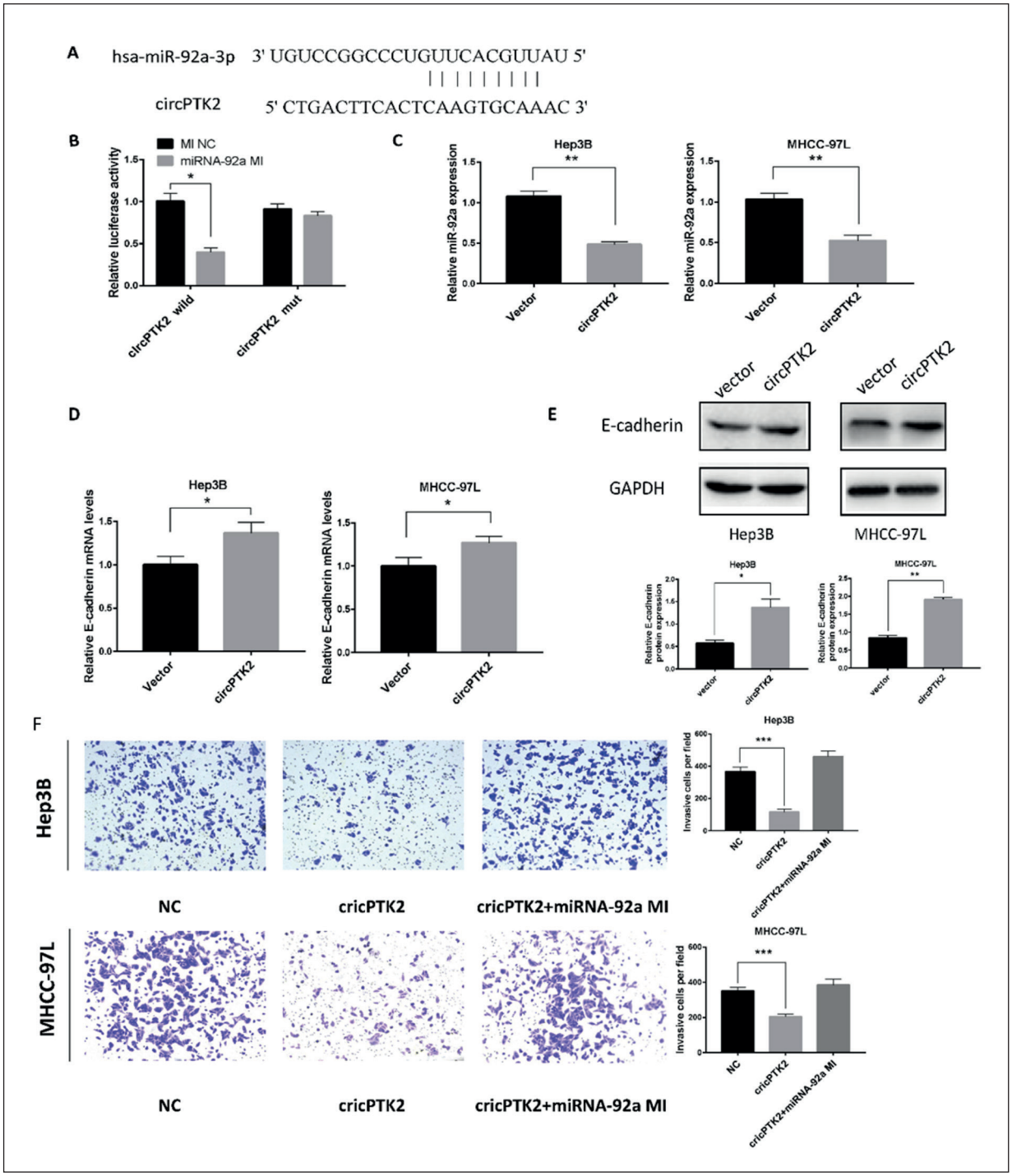

Figure 4. CircPTK2 directly binds to miR-92a in HCC cells. **A,** Potential binding sites of circPTK2 and miR-92a. **B,** Dual-Luciferase reporter gene assay in 293T cells cotransfected with wild type/mutant circPTK2 and miR-92a mimic/negative control. **C,** Expression level of miR-92a in Hep3B cells transfected with vector and circPTK2 overexpression plasmid via qRT-PCR. **D,** Expression of E-cadherin in Hep3B cells transfected with empty vector or circPTK2 overexpression plasmid was measured via qRT-PCR. **E,** Western blot analysis of E-cadherin expression in Hep3B cells transfected with empty vector or circPTK2 overexpression plasmid. **F,** Effect of vector, circPTK2 overexpression, and miR-92a-3p mimic on the invasion of Hep3B and MHCC-97L cells (200×). *p <0.05; **p < 0.01; ***p < 0.001.

expression of E-cadherin in liver cancer cells by acting as a ceRNA to inhibit the expression of miR-92a.

The Effect of MiR-92a in HCC Cells is Abolished by CircPTK2

To understand the underlying effects of miR-92a on cell invasion mediated by circPTK2, transwell assays were performed. These studies revealed that circPTK2 suppressed invasion ability, which was induced by miR-92a. These observations indicated that the effects of miR-92a on HCC cell invasion can be reversed by circPTK2 (Figure 4F).

Discussion

First, we found that miR-92a was upregulated in HCC cells and tissues. In addition, Luciferase reporter assays showed that circPTK2 and the E-cadherin 3′UTR have the same miR-92a response elements and may therefore competitively bind to miR-92a. Indeed, further studies suggested that circPTK2 regulates E-cadherin levels by sponging to miR-92a expression.

Abnormal expression of miR-92a has been reported in many types of cancer, including lung cancer, colorectal cancer, and acute granulocyte lymphoma[9,16-18]. Wu et al[19] have shown that the expression of miR-92a is significantly higher in CRC tissues compared with adjacent tissues and in patients' plasma. Furthermore, upregulating miR-92a influences the metastatic potential of non-small-cell lung cancer through the PTEN/PI3K/AKT axis[20]. We found that miR-92a was upregulated in HCC cells and significantly increased HCC cell proliferation and invasion. Recently, a significant body of evidence has revealed that a ceRNA regulatory network is involved in the development of HCC[21-24]. Differentiation antagonizing non-protein coding RNA (lncRNA DANCR) acts as a ceRNA to inhibit miR-27a-3p by affecting the ROCK1/LIMK1/COFILIN1 pathway in HCC cells[24]. Furthermore, circFBLIM1 directly targets miR-346 and acts as a competing endogenous RNA (ceRNA) to regulate FBLIM1 expression to exert regulatory functions in HCC[23]. Since circRNAs work by binding to miRNAs, we wanted to determine whether circRNAs could act as a sponge for miR-92a. Bioinformatics analysis predicted that miR-92a and circPTK2 shared similar binding sites. In addition, circPTK2 has been shown to repress the invasion of non-small cell lung cancer cells[25]. We thus investigated the effect of circPTK2 on HCC cell lines and found that overexpression of circPTK2 greatly inhibited HCC cell invasion.

Epithelial-mesenchymal transition (EMT) is a crucial event in the progression of cancer metastasis[26-28]. EMT triggers cellular mobility and induces the invasion of tumor cells[29]. The most prominent characteristic of an EMT event is decreased expression of epithelial markers such as E-cadherin and increased expression of mesenchymal markers such as N-cadherin and vimentin[30-33]. We found that miR-92a targets the E-cadherin 3'UTR and silence E-cadherins at the post-transcriptional level. Results of qRT-PCR and Western blotting confirmed that miR-92a decreased the expression of E-cadherin and increased MMP2, vimentin, MMP9, N-cadherin, and CLDN4. The downregulation of E-cadherin, however, was rescued by circPTK2. In summary, we found that overexpression of miR-92a enhanced proliferation and invasion by targeting the E-cadherin 3′UTR in HCC cells. In addition, we demonstrated that circPTK2 played a role as a sponge of miR-92a in HCC cells. This study expands our understanding of the circPTK2/miR-92a/E-cadherin regulatory axis. The expression of miR-92a should be considered a potential biomarker and therapeutic target against HCC metastasis.

Conclusions

Our results suggested that miR-92a can enhance the proliferation and invasion of HCC cells by inhibiting E-cadherin; however, these effects can be blocked by circPTK2.

Conflict of Interest

The Authors declare that they have no conflict of interests.

Acknowledgements

This work was supported by the National Natural Science Foundation of China (grant number: 81430041, 81620108017, 81771879, 81871462) and Natural Science Foundation of Guangdong Province (2019A1515011223).

References

1) Bray F, Ferlay J, Soerjomataram I, Siegel RL, Torre LA, Jemal A. Global cancer statistics 2018. GLOBOCAN estimates of incidence and mortality worldwide for 36 cancers in 185 countries. CA Cancer J Clin 2018; 68: 394-424.

2) Tsai JH, Yang J. Epithelial-mesenchymal plasticity in carcinoma metastasis. Genes Dev 2013; 27: 2192-2206.

3) Hayes J, Peruzzi PP, Lawler S. MicroRNAs in cancer. biomarkers, functions and therapy. Trends Mol Med 2014; 20: 460-469.

4) Yu J, Xie F, Bao X, Chen W, Xu Q. miR-300 inhibits epithelial to mesenchymal transition and metastasis by targeting Twist in human epithelial cancer. Mol Cancer 2014; 13: 121.

5) Adams BD, Parsons C, Walker L, Zhang WC, Slack FJ. Targeting noncoding RNAs in disease. J Clin Invest 2017; 127: 761-771.

6) Baek D, Villen J, Shin C, Camargo FD, Gygi SP, Bartel DP. The impact of microRNAs on protein output. Nature 2008; 455: 64-71.

7) Karreth FA, Reschke M, Ruocco A, Ng C, Chapuy B, Leopold V, Sjoberg M, Keane TM, Verma A, Ala U, Tay Y, Wu D, Seitzer N, Velasco-Herrera Mdel C, Bothmer A, Fung J, Langellotto F, Rodig SJ, Elemento O, Shipp MA, Adams DJ, Chiarle R, Pandolfi PP. The BRAF pseudogene functions as a competitive endogenous RNA and induces lymphoma in vivo. Cell 2015; 161: 319-332.

8) Thomson DW, Dinger ME. Endogenous microRNA sponges. evidence and controversy. Nat Rev Genet 2016; 17: 272-283.

9) Tsuchida A, Ohno S, Wu W, Borjigin N, Fujita K, Aoki T, Ueda S, Takanashi M, Kuroda M. miR-92 is a key oncogenic component of the miR-17-92 cluster in colon cancer. Cancer Sci 2011; 102: 2264-2271.

10) Mandal M, Myers JN, Lippman SM, Johnson FM, Williams MD, Rayala S, Ohshiro K, Rosenthal DI, Weber RS, Gallick GE, El-Naggar AK. Epithelial to mesenchymal transition in head and neck squamous carcinoma. association of Src activation with E-cadherin down-regulation, vimentin expression, and aggressive tumor features. Cancer 2008; 112: 2088-2100.

11) Labernadie A, Kato T, Brugues A, Serra-Picamal X, Derzsi S, Arwert E, Weston A, Gonzalez-Tarrago V, Elosegui-Artola A, Albertazzi L, Alcaraz J, Roca-Cusachs P, Sahai E, Trepat X. A mechanically active heterotypic E-cadherin/N-cadherin adhesion enables fibroblasts to drive cancer cell invasion. Nat Cell Biol 2017; 19: 224-237.

12) Nieto MA, Huang RY, Jackson RA, Thiery JP. EMT. 2016. Cell 2016; 166: 21-45.

13) Zhu Y, Yan L, Zhu W, Song X, Yang G, Wang S. MMP2/3 promote the growth and migration of laryngeal squamous cell carcinoma via PI3K/Akt-NF-kappaB-mediated epithelial-mesenchymal transformation. J Cell Physiol 2019.

14) Wen SL, Gao JH, Yang WJ, Lu YY, Tong H, Huang ZY, Liu ZX, Tang CW. Celecoxib attenuates hepatic cirrhosis through inhibition of epithelial-to-mesenchymal transition of hepatocytes. J Gastroenterol Hepatol 2014; 29: 1932-1942.

15) Hwang TL, Lee LY, Wang CC, Liang Y, Huang SF, Wu CM. Claudin-4 expression is associated with tumor invasion, MMP-2 and MMP-9 expression in gastric cancer. Exp Ther Med 2010; 1: 789-797.

16) Chen E, Li Q, Wang H, Yang F, Min L, Yang J. MiR-92a promotes tumorigenesis of colorectal cancer, a transcriptomic and functional based study. Biomed Pharmacother 2018; 106: 1370-1377.

17) Concepcion CP, Bonetti C, Ventura A. The microRNA-17-92 family of microRNA clusters in development and disease. Cancer J 2012; 18: 262-267.

18) Mendell JT. miRiad roles for the miR-17-92 cluster in development and disease. Cell 2008; 133: 217-222.

19) Wu CW, Ng SS, Dong YJ, Ng SC, Leung WW, Lee CW, Wong YN, Chan FK, Yu J, Sung JJ. Detection of miR-92a and miR-21 in stool samples as potential screening biomarkers for colorectal cancer and polyps. Gut 2012; 61: 739-745.

20) Ren P, Gong F, Zhang Y, Jiang J, Zhang H. MicroRNA-92a promotes growth, metastasis, and chemoresistance in non-small cell lung cancer cells by targeting PTEN. Tumour Biol 2016; 37: 3215-3225.

21) Wang Y, Yang L, Chen T, Liu X, Guo Y, Zhu Q, Tong X, Yang W, Xu Q, Huang D, Tu K. A novel lncRNA MCM3AP-AS1 promotes the growth of hepatocellular carcinoma by targeting miR-194-5p/FOXA1 axis. Mol Cancer 2019; 18: 28.

22) Xiong DD, Dang YW, Lin P, Wen DY, He RQ, Luo DZ, Feng ZB, Chen G. A circRNA-miRNA-mRNA network identification for exploring underlying pathogenesis and therapy strategy of hepatocellular carcinoma. J Transl Med 2018; 16: 220.

23) Bai N, Peng E, Qiu X, Lyu N, Zhang Z, Tao Y, Li X, Wang Z. circFBLIM1 act as a ceRNA to promote hepatocellular cancer progression by sponging miR-346. J Exp Clin Cancer Res 2018; 37: 172.

24) Guo D, Li Y, Chen Y, Zhang D, Wang X, Lu G, Ren M, Lu X, He S. DANCR promotes HCC progression and regulates EMT by sponging miR-27a-3p via ROCK1/LIMK1/COFILIN1 pathway. Cell Prolif 2019; 52: e12628.

25) Wang L, Tong X, Zhou Z, Wang S, Lei Z, Zhang T, Liu Z, Zeng Y, Li C, Zhao J, Su Z, Zhang C, Liu X, Xu G, Zhang HT. Circular RNA hsa_circ_0008305 (circPTK2) inhibits TGF-beta-induced epithelial-mesenchymal transition and metastasis by controlling TIF1gamma in non-small cell lung cancer. Mol Cancer 2018; 17: 140.

26) Lin L, Cheng K, He Z, Lin Q, Huang Y, Chen C, Xie Z, Chen L, Liang Z. A polysaccharide from Hedyotis diffusa interrupts metastatic potential of lung adenocarcinoma A549 cells by inhibiting EMT via EGFR/Akt/ERK signaling pathways. Int J Biol Macromol 2019; 129: 706-714.

27) Wang L, Yang G, Zhao D, Wang J, Bai Y, Peng Q, Wang H, Fang R, Chen G, Wang Z, Wang K, Li G, Yang Y, Wang Z, Guo P, Peng L, Hou D, Xu W. CD103-positive CSC exosome promotes EMT of clear cell renal cell carcinoma. role of remote MiR-19b-3p. Mol Cancer 2019; 18: 86.

28) Huang J, Lo UG, Wu S, Wang B, Pong RC, Lai CH, Lin H, He D, Hsieh JT, Wu K. The roles and mechanism of IFIT5 in bladder cancer epithelial-mesenchymal transition and progression. Cell Death Dis 2019; 10: 437.

29) Wang J, Zhang Z, Li R, Mao F, Sun W, Chen J, Zhang H, Bartsch JW, Shu K, Lei T. ADAM12 induces EMT and promotes cell migration, invasion and proliferation in pituitary adenomas via EGFR/ERK signaling pathway. Biomed Pharmacother 2018; 97: 1066-1077.

30) Kohler I, Bronsert P, Timme S, Werner M, Brabletz T, Hopt UT, Schilling O, Bausch D, Keck T, Wellner UF. Detailed analysis of epithelial-mesenchymal transition and tumor budding identifies predictors of long-term survival in pancreatic ductal adenocarcinoma. J Gastroenterol Hepatol 2015; 30: 78-84.

31) Kim WK, Byun WS, Chung HJ, Oh J, Park HJ, Choi JS, Lee SK. Esculetin suppresses tumor growth and metastasis by targeting Axin2/E-cadherin axis in colorectal cancer. Biochem Pharmacol 2018; 152: 71-83.

32) Hou J, Yan J, Ren XY, Zhu K, Du XY, Li JJ, Xu M. Long noncoding RNA ROR1-AS1 induces tumor metastasis and epithelial-mesenchymal transition by sponging miR-375 in nasopharyngeal carcinoma. Eur Rev Med Pharmacol Sci 2020; 24: 174-180.

33) Chen WL, Jiang L, Wang JS, Liao CX. Circ-0001801 contributes to cell proliferation, migration, invasion and epithelial to mesenchymal transition (EMT) in glioblastoma by regulating miR-628-5p/HMGB3 axis. Eur Rev Med Pharmacol Sci 2019; 23: 10874-10885.